

Synthesis and Characterization of Polyimide-Cobalt Ferrite Nanocomposites

D. Mazuera^{*}, Y. Cedeño-Mattei^{**}, O. Perales-Perez^{***}, and S. P. Singh^{***}

^{*}University of Puerto Rico, Department of Mechanical Engineering, Mayagüez, Puerto Rico 00681

^{**}University of Puerto Rico, Department of Chemistry, Mayagüez, Puerto Rico 00681

^{***}University of Puerto Rico, Department of Engineering Science and Materials, Mayaguez, Puerto Rico 00680-9044

ABSTRACT

Magnetic nanocrystals exhibiting outstanding coercivity values can be dispersed in polymer-based composites for use in micro actuators, micro pumps and sensing devices. In the present work, cobalt ferrite nanocrystals were synthesized under size-controlled conditions in aqueous phase and incorporated into a polyimide matrix at various volumetric loads. Synthesized 20nm-cobalt ferrite single crystals, which exhibited a coercivity of 2.9kOe at room-temperature, were dispersed in polyimide precursor (Dupont PI2555) and cured to develop the polyimide matrix in the resulting nanocomposites. Produced films were characterized by Fourier transform infrared spectroscopy, X-ray diffraction and vibrating sample magnetometry, which confirmed the formation of the nanocomposite. As expected, the saturation magnetization in the nanocomposites varied according to the Polyimide/Ferrite weight ratio, while coercivity remained at the value corresponding to pure cobalt ferrite nanocrystals.

Keywords: PMC, magnetic nanocomposite, cobalt ferrite, polyimide.

1 INTRODUCTION

Organic-inorganic magnetic nanocomposites, also known as ‘magnetic polymers’, are of particular scientific and technological interest due to their wide range of actual and potential applications in polymer bonded magnets, micro electro mechanical systems (MEMS), micro sensors, high density storage and magneto optical media, electromagnetic shielding, cell separation, medical diagnosis, and others [1-15]. Reasons for this increasing importance include the relative low cost of these nanocomposites in comparison to metallic or ceramic conventional magnets, simplicity of their synthesis and forming and outstanding magnetic properties due to nanometric size of the dispersoids (critical factor to manufacture micro or macro scaled devices) coupled with the flexibility of light polymer matrices [9, 16]. Magnetic properties of cobalt ferrite nanoparticles can be tuned by restricting their crystallite size within the single domain region. This control of the crystal size is conducive to outstanding values of coercivity in comparison to the bulk value. In this work, 20nm-cobalt ferrite single domain

crystals, exhibiting room-temperature coercivity of 2.9kOe, were synthesized in aqueous phase under size-controlled conditions and used as dispersoids in polyimide, PI, matrix to produce nanocomposite films. The selection of the PI matrix is based on its suitable mechanical strength as required for the development of polymer magnets and related devices [3, 10, 13, 18]. The PI-cobalt ferrite nanocomposites were synthesized at two volumetric loads of the disperse phase (10% v/v and 20% v/v) and characterized on a structural and magnetic basis.

2 EXPERIMENTAL

2.1 Materials

All reagents were of analytical grade and were used without further purification. Required weights of chloride salts of Fe(III) and Co(II) ions were dissolved in distilled water to achieve a mole ratio Fe/Co of two. NaOH was used as the precipitant. Dupont PI2555, a benzophenone tetra-carboxylic dianhydride-oxydianiline-metaphenylene diamine formulation containing 20% of polyamic acid, was used as polyimide precursor. Isopropyl trisostearyl titanate (Kenrich Petrochemicals KR-TTS) was used to improve dispersion of inorganic nanoparticles in the polymeric matrix. This dispersant reacts with free protons at the nanoparticle surface to form an organic-titanium monomolecular coating layer [3].

2.2 Synthesis of Cobalt Ferrite Nanocrystals

Cobalt ferrite nanocrystals were synthesized by a modified coprecipitation method. An aqueous solution of 0.11M Fe(III) and 0.55M Co(II) was continuously added with controlled flow rate of 1ml/min to the reaction vessel containing an aqueous solution of 0.48M NaOH under boiling conditions. The vessel was kept under heating conditions for one hour to allow dehydration and atomic rearrangement involved with the conversion of the intermediate hydroxide into the ferrite crystalline structure. Ferrite nanocrystals were magnetically recovered, washed thoroughly three times with distilled water and dried for 24 hours at 80°C [17]. Figure 1 shows the high resolution transmission electron microscope (HRTEM) image of the ferrite nanocrystals used in this study.

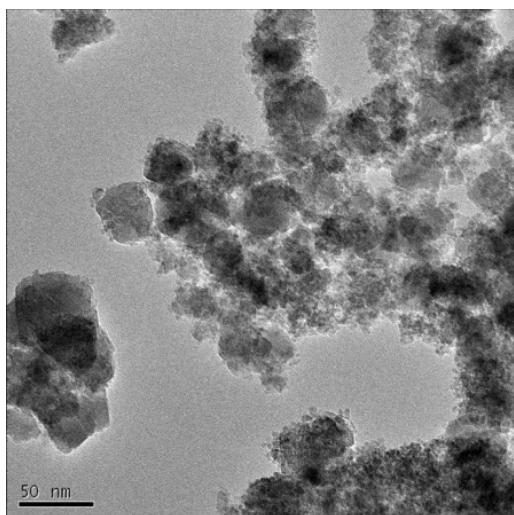


Figure 1. HRTEM image of cobalt ferrite nanocrystals synthesized according to reference [17]

2.3 Synthesis of Polyimide-Cobalt Ferrite Nanocomposites

Thirty milliliters of polyimide precursor (Dupont PI2555) was mixed with 741 μ l of the KR-TTR dispersant. Suitable amounts of ferrite powder were added to the previous solution to achieve the desired volumetric loads (10% and 20%). These volumetric loads were calculated based on the average solids content of PI2555 precursor and the theoretical densities of pure PI and cobalt ferrite [3, 17]. The ferrite-polymer precursor solution was mixed using an IKA T18 homogenizer (with S18N-19G dispersing tool) for 1 hour of contact at 10,000 RPM.

Solvent-cast free-standing films of polyimide and the corresponding composites were prepared by pouring 0.6 to 1 ml of the precursor solution into a mold consisting of a glass substrate and a stainless steel ring (29.4 mm in diameter). The mold containing the precursor solution was heated at 85°C until all solvent was removed. Produced films were peeled out from the substrate and thermally cured. This curing process was carried out by the following sequence: (i) heating of the films from room temperature to 200°C at a 4°C/min rate; (ii) 30 minutes of heating at 200°C; (iii) heating up to 300°C at 2.5°C/min; (iv) dwelling during 60 minutes; and (v) cooling down inside the furnace. The whole curing cycle took place in a 99.998% nitrogen atmosphere. The film thickness obtained ranged from 100 μ m to 150 μ m. Figure 2 shows the images of pure PI and 10%v/v composite films at 10X magnification.

2.4 Materials Characterization

Structural analyses of films and powders were carried out using the Cu-K α radiation in a Siemens D500 x-ray diffractometer (XRD). Fourier-transform infrared (FTIR) spectroscopy was also used to confirm the structure of the

matrix in the developed composites. FTIR spectra were obtained in a Scimitar FTS 2000 Digilab spectrometer. The variation in magnetization and coercivity of the nanocomposites with the volumetric load of the disperse phase was determined by room-temperature magnetization measurements in a Lake Shore-7400 vibrating sample magnetometer (VSM) unit.



Figure 2. Stereo images of pure PI film, (a), and 10% v/v ferrite nanocomposite film, (b).

3 RESULTS AND DISCUSSION

3.1 FTIR Analyses

Figure 3 shows the FTIR spectra for pure polyimide and nanocomposite films containing 10% v/v and 20% v/v of cobalt ferrite nanoparticles. The bands at 1780 cm^{-1} (C=O asymmetrical stretching), 1710 cm^{-1} (C=O symmetrical stretching), 1370 cm^{-1} (C-N stretching) and 710 cm^{-1} (C=O bending) can be assigned to imide groups in the polyimide structure. In turn, the absence of bands in the 3200 cm^{-1} - 2900 cm^{-1} range suggests the completion of the imidization process by removal of H and OH species from the structure of the polyamic acid.

3.2 XRD Analyses

XRD analyses of the polyimide matrix, isolated disperse cobalt ferrite nanoparticles and corresponding nanocomposites confirmed the formation of expected structures. Only well-defined peaks corresponding to the ferrite structure were observed for the disperse phase (Figure 4-b). The corresponding average crystallite size and lattice parameter were estimated to be 20 nm and 8.34 \AA , respectively. These values are in good agreement with those reported by Y. Cedeño *et al.* in earlier publications [17]. The broad XRD peak centered on 18° in bare polyimide films (Figure 4-a) indicates a short-range molecular order, which is also encountered in the 10% v/v nanocomposite but located at a lower diffraction angle (Figure 4-c). This shift in 2 θ value indicates an increase of the interplanar distance in the polymer that could be attributed to the close interaction between polymer chains and incorporated ferrite

nanocrystals. The molecular ordering in the polymeric matrix was no longer evident when the volume fraction of ferrite in the nanocomposite was increased to 20%; the incorporation of ferrite nanoparticles in the composite would have inhibited the development and/or ordering of the polymeric chains.

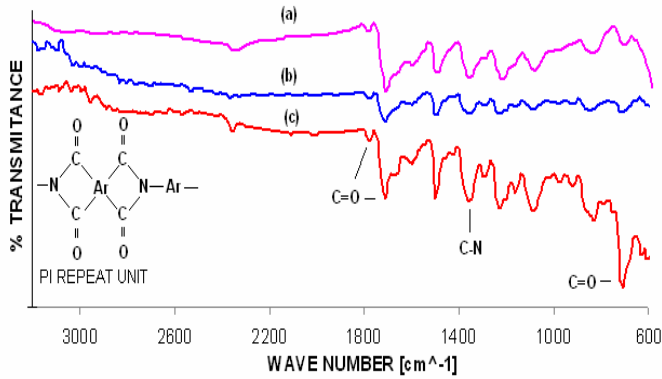


Figure 3. FTIR spectra for 20%v/v ferrite composite, (a); 10% v/v ferrite composite, (b); and bare polyimide films (c)

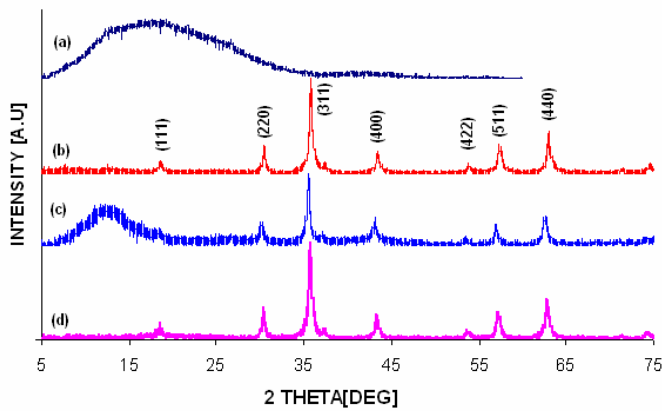


Figure 4. XRD patterns for pure polyimide film, (a); cobalt ferrite powders, (b); 10% v/v ferrite composite film, (c); and 20%v/v ferrite composite film, (d).

3.3 Magnetic Measurements

Room-temperature M-H loops for isolated ferrite nanoparticles and nanocomposite films synthesized at 10% v/v and 20% of ferrite volumetric loads are shown in Figure 5 and Figure 6, respectively. The maximum magnetization of pure cobalt ferrite powders was 42.5emu/g; the lack of saturation in the corresponding M-H loop can be attributed to the significant presence of superparamagnetic particles in the polydisperse powders. In turn, the saturation magnetization observed in the M-H loops for the nanocomposites films can be a

consequence of the immobilization of the ferrite nanocrystals in the polymeric matrix. The saturation magnetization of the nanocomposites varied from 13emu/g to 25emu/g when the ferrite volumetric load was increased from 10% to 20%. As expected, the coercivity remained constant (2.9kOe) in both samples. In order to verify the isotropic behavior of the composite films, their M-H loops were measured by applying the magnetic field along parallel (Figure 5-a and 6-a) and perpendicular (Figure 5-b and 6-b) directions with respect to film surface. The small variation in both, the saturation magnetization and coercivity with the direction at which the external magnetic field was applied suggests the formation of isotropic magnetic nanocomposite films.

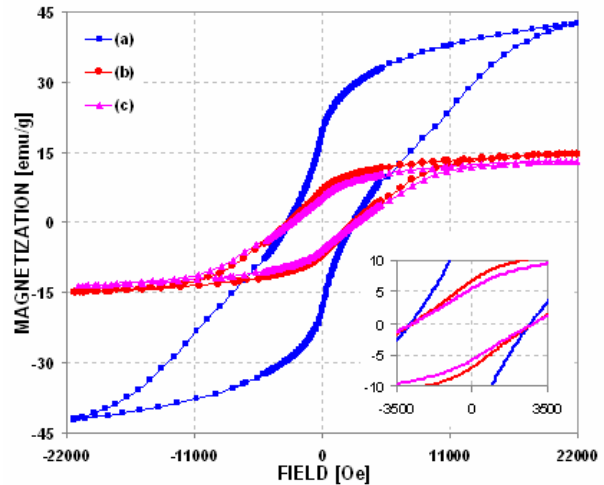


Figure 5. Room temperature M-H loops for cobalt ferrite powders, (a), and 10% v/v ferrite composite film measured along parallel, (b), and transverse direction, (c), with respect to film surface. The inset shows the M-H data around the origin.

4 CONCLUDING REMARKS

We have synthesized polyimide-cobalt ferrite nanocomposite films having well-tuned magnetic properties. As suggested by the structural characterization of produced films, the inclusion of ferrite nanoparticles in the polyimide matrix would inhibit the development and/or ordering of the polymeric chains. Although the magnetization of the nanocomposites was found to be strongly dependent on the volumetric load of the ferrite nanoparticles, the corresponding coercivity remained constant. M-H measurements also evidenced the isotropic magnetic behavior exhibited by the nanocomposite films. Ongoing works are focused on the study of the thermo-mechanical behavior of bare polyimide and magnetic nanocomposite films.

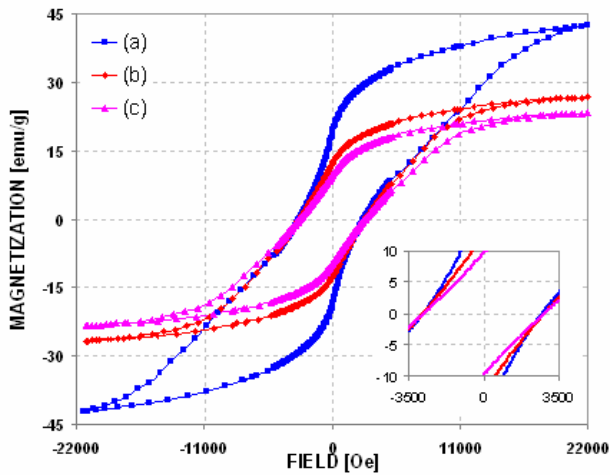


Figure 6. Room temperature M-H loops for cobalt ferrite powders, (a), and 20% v/v ferrite composite film measured along the parallel, (b), and transverse direction, (c), with respect to film surface. The inset shows the M-H data around the origin.

AKNOWLEDGMENTS

This material was based upon work supported by the National Science Foundation under award N° DMR.0351449 (PREM Program). Thanks are also extended to Kenrich Petrochemicals and HD Microsystems for assistance and technical support. One of the authors (YCM) also acknowledges the support received by the Institute of Functional Nanomaterials of Puerto Rico.

REFERENCES

[1] Tsung-Shune Chin, *Journal of Magnetism and Magnetic Materials*, 209, 75-79, 2000.
 [2] L. García-Cerda, M. Escareño-Castro, M. Salazar-Zertuche, *Journal of Non-Crystalline Solids*, 353, 808-810, 2007.
 [3] L. Lagorce, M. Allen, *Journal of Microelectromechanical Systems*, vol. 6, no. 4, 307-312, 1997.
 [4] K. Baba, F. Takase, M. Miyagi, *Optics Communications*, 139, 35-38, 1997.
 [5] S. Spearing, *Acta Materialia*, 48, 179-196, 2000.
 [6] C. P. Sasso, M. Pasquale, L. Giudici, S. H. Lim, S.M. Na, *Sensors and Actuators*, 129, 159-162, 2006.
 [7] A. Voigt, M. Heinrich, C. Martin, A. Llobera, G. Gruetzner, F. Pérez-Murano, *Microelectronic Engineering*, 84, 1075-1079, 2007.

[8] S. Sindhua, S. Jegadesanb, A. Parthiban, S. Valiyaveetil, *Journal of Magnetism and Magnetic Materials*, 296, 104-113, 2006.
 [9] M. Makleda, T. Matsuib, H. Tsudab, H. Mabuchib, M. El-Mansya, K. Morii, *Journal of Materials Processing Technology*, 160, 229-233, 2005.
 [10] S. K. Lim, K. J. Chung, Y. Kim, C. K. Kim, C.S. Yoon, *Journal of Colloid and Interface Science*, 273, 517-522, 2004.
 [11] I. G. Yanez-Flores, R. Betancourt-Galindo, J. A. Matutes Aquino, O. Rodriguez-Fernandez, *Journal of Non-Crystalline Solids*, 353, 799-801, 2007.
 [12] J. H. Kim, J. Kim, K. H. Baek, D. H. Im, C. K. Kim, C. S. Yoon, *Colloids and Surfaces A: Physicochem. Eng. Aspects*, 301, 419-424, 2007.
 [13] J. Zhan, G. Tian, L. Jiang, Z. Wu, D. Wu, X. Yang, R. Jin, *Thin Solid Films*, 916, 6315-6320 2008.
 [14] J. Slama, A. Gruskova, R. Vıcen, S. Vıcenova, R. Dosoudil, J. Franek, *Journal of Magnetism and Magnetic Materials*, 254-255, 642-645, 2003
 [15] M. Pasquale, C. P. Sasso, M. Velluto, S. H. Lim, S.H, *Journal of Magnetism and Magnetic Materials*, 242-245, 1460-1463, 2002.
 [16] D. Askeland, P. Phule, *The Science and Engineering of Materials*, Fifth Edition, Thomson, 2005.
 [17] Y. Cedeño-Mattei, O. Perales-Pérez, M. Tomar, F. Román, *Journal of Applied Physics*, 103, 07e512, 2008.
 [18] P. M. Ajayan, L. S. Schadler, P. V. Braun, *Nanocomposite Science and Technology Wiley-Vch*, 2003.